



Harmonic analysis and distribution-free inference for spherical distributions

S. Rao Jammalamadaka^a, György H. Terdik^{b,*}

^a Department of Statistics and Applied Probability, University of California, Santa Barbara, CA 93106, USA

^b Faculty of Informatics, University of Debrecen, 4028 Debrecen, Hungary



ARTICLE INFO

Article history:

Received 23 February 2018

Available online 4 February 2019

AMS 2008 subject classifications:

primary 62H11

62H15

secondary 60E05

60E10

Keywords:

Dimroth–Watson distribution

Harmonic analysis

Large-sample tests

Spherical distributions

Symmetries of densities

Three-dimensional directional data

Von mises–fisher distribution

ABSTRACT

Fourier analysis, and representation of circular distributions in terms of their Fourier coefficients, is quite commonly discussed and used for model-free inference such as testing uniformity and symmetry, in dealing with 2-dimensional directions. However, a similar discussion for spherical distributions, which are used to model 3-dimensional directional data, is not readily available in the literature in terms of their harmonics. This paper, in what we believe is the first such attempt, looks at probability distributions on a unit sphere through the perspective of spherical harmonics, analogous to the Fourier analysis for distributions on a unit circle. Representation of any continuous spherical density in terms of spherical harmonics is given, and such series expansions provided for some commonly used spherical distributions, as well as for two new spherical distributions that are introduced. Through the prism of harmonic analysis, one can look at the mean direction, dispersion, and various forms of symmetry for these models in a nonparametric setting. Aspects of distribution-free inference such as estimation and large-sample tests for various symmetries, are provided, each type of symmetry being characterized through its harmonics. The paper concludes with a real-data example analyzing the longitudinal sunspot activity.

© 2019 Elsevier Inc. All rights reserved.

1. Introduction

Probability models for directional data in two and three dimensions can be represented using the circumference of a unit circle and the surface of a unit sphere as the support; they are called circular and spherical distributions, respectively. In any discussion of probability distributions on the circle, Fourier analysis becomes an integral part, because such probability densities on a circle are periodic with period 2π ; see, e.g., Section 2.1 in [30] or Section 3.3.2 in [23]. When it comes to directions in three dimensions and probability distributions on the sphere, however, similar treatment is nearly absent, partly because of the complexity, as we shall soon see. Yet, in spite of this complexity, such a study of spherical distributions through their harmonics lets one probe deeper into their fundamental properties and characterize their behavior in terms, e.g., of their symmetries in a general model-free setting rather than by dealing with specific parametric models. We note that topics such as density estimation [15], testing symmetry under a given group of isometries [17], testing uniformity [11,16] have been considered in the general setting of a Riemannian manifold. More direct use of spherical harmonics is made by Healy et al. [14] and Kim et al. [19], who consider nonparametric deconvolution of spherical densities, and by Lacour and Ngoc [22], who study goodness-of-fit for noisy directional data.

* Corresponding author.

E-mail addresses: rao@pstat.ucsb.edu (S.R. Jammalamadaka), Terdik.Gyorgy@inf.unideb.hu (Gy.H. Terdik).

It is our goal in this paper to focus on harmonic analysis of spherical distributions in a general setting, and to provide model-free large-sample procedures for testing various symmetries that these distributions might enjoy, but all from the perspective of their harmonic representations and the properties of resulting coefficients.

Harmonics play an important role in geosciences where they serve the role of smoothing and interpolation for noisy data sets. A good example of this is the map of global heat flow presented in [6]; see also [10] where spatio-temporal data on global climate are presented through visual animations. In the case of gravity and magnetic fields, among others, spherical harmonics are the solutions to differential equations that govern the potentials and provide a deeper physical relationship to the fields. Additional applications for such analysis include computational geometry [18], image processing [32], approximate symmetries in a large data set [20], “big data” analytics for meteorological data sets [21].

The paper is organized as follows. In Section 2, we start with a brief introduction to the basis set for spherical harmonics and some properties. This section then provides the important series expansion for any spherical density in terms of its harmonics. Much of the mathematical machinery needed for the paper can be found in Appendix A. In Section 3, some well-known parametric models for the unit sphere that have been commonly used in the literature to model 3-dimensional directional data, are presented along with their series expansion in terms of spherical harmonics. We also introduce here two new spherical models.

Section 4 provides harmonic representations for the mean direction and dispersion for such spherical models. Section 5 discusses estimation of the harmonic coefficients, the mean direction, and the covariance structure. Various forms of symmetry that a spherical distribution might enjoy, such as isotropy, antipodal symmetry, and rotational symmetry are discussed in Section 6 along with omnibus large-sample tests for these various forms of symmetry. Any particular type of symmetry may be characterized in terms of the properties of the harmonic coefficients in the series expansion of a density, and thus help us to focus more effectively in checking for that specific type of symmetry. Among such tests, although testing uniformity in particular has been rather well studied, and may be viewed as a special case of such results for a Riemannian manifold [11,16], our test statistic takes a simple form as finite unweighted sum of squares of the harmonic coefficients, and comes directly from the particular characterization of uniformity. Similarly in the context of testing symmetry under given isometries, Jupp and Spurr [17] use randomization tests, while we propose a large-sample test based on the asymptotic null distribution. Our methodology of working with the harmonic coefficients allows for testing various other forms of symmetry, as outlined in this section. The final section deals with a real data example on sunspot activity, and Appendix B provides a few important proofs.

For a more practical and computational side of these issues, the reader is referred to a companion paper [34] together with a MATLAB package entitled “3D-Directional Statistics, Simulation and Visualization (3D-Directional-SSV)” by the authors, which provides various simulation techniques and visualization tools for spherical models.

2. Spherical harmonics and probability distributions on the unit sphere

Continuous functions on a compact set can usually be approximated uniformly by an orthogonal system of basis functions. In particular, we consider the unit sphere in 3-dimensions, labeled the 2D-Sphere \mathbb{S}_2 which is a compact set in \mathbb{R}^3 , with co-latitude $\vartheta \in [0, \pi]$ and longitude $\varphi \in [0, 2\pi]$. Continuous functions on such a sphere can be approximated uniformly by sums of orthonormal spherical harmonic; see, e.g., Theorem 9 in [25]. Such a basis set for \mathbb{S}_2 is given by the complex-valued functions $\{Y_\ell^m(\vartheta, \varphi) : \ell = 0, \dots, \infty, m = -\ell, \dots, \ell\}$ of degree ℓ and order m , defined, for all $\varphi \in [0, 2\pi]$ and $\vartheta \in [0, \pi]$, by

$$Y_\ell^m(\vartheta, \varphi) = (-1)^m \sqrt{\frac{2\ell + 1}{4\pi} \frac{(\ell - m)!}{(\ell + m)!}} P_\ell^m(\cos \vartheta) e^{im\varphi}, \quad (1)$$

where P_ℓ^m denotes associated normalized Legendre function of the first kind; see Section 3.2 in [7].

These Y_ℓ^m 's are normalized in the sense that, for each ℓ and m ,

$$\int_0^{2\pi} \int_0^\pi |Y_\ell^m(\vartheta, \varphi)|^2 \sin \vartheta d\vartheta d\varphi = 1.$$

When $\mathbf{x}(\vartheta, \varphi)$ denotes a point on the unit sphere \mathbb{S}_2 , we shall use the alternate notation $Y_\ell^m(\mathbf{x})$ in place of $Y_\ell^m(\vartheta, \varphi)$. The spherical harmonics of order 0 have a special form so that for each ℓ ,

$$Y_\ell^0(\vartheta, \varphi) = \sqrt{\frac{2\ell + 1}{4\pi}} P_\ell(\cos \vartheta). \quad (2)$$

where P_ℓ denotes the Legendre polynomial.

Spherical harmonics are in general complex-valued because they depend on $e^{im\varphi}$, where φ is the longitude. Clearly $e^{im\varphi}$ is equivalent to the real-valued sine–cosine system, splitting which, we can define real spherical harmonic functions (note the double subscripts)

$$Y_{\ell,m} = \begin{cases} \{Y_\ell^m + (-1)^m Y_\ell^{-m}\} / \sqrt{2} & \text{if } m > 0, \\ Y_\ell^0 & \text{if } m = 0, \\ \{Y_\ell^{-m} - (-1)^m Y_\ell^m\} / (i\sqrt{2}) & \text{if } m < 0. \end{cases}$$

The harmonics for $m > 0$ are said to be of the cosine type, while those for $m < 0$ are of the sine type. Although, as in Fourier analysis, complex-valued harmonics can be re-expressed in terms of real-valued harmonics which often provide somewhat simpler expressions in many cases, we will develop the basic theory here using the complex-valued spherical harmonics.

We refer the reader to [Appendix A](#) and to [31,35] for a more detailed account of spherical harmonics.

2.1. Probability distributions on a unit sphere and their harmonic representation

Let f denote a density function corresponding to a spherical distribution on the unit sphere \mathbb{S}_2 . Denoting by $\Omega(d\omega)$ the Lebesgue element of the surface area on \mathbb{S}_2 , we have the following result.

Theorem 1 ([25], p. 40). *When the density function f is continuous, it has the following series expansion in terms of the spherical harmonics Y_ℓ^m :*

$$f(\mathbf{x}) = \sum_{\ell=0}^{\infty} \sum_{m=-\ell}^{\ell} a_\ell^m Y_\ell^m(\mathbf{x}), \tag{3}$$

where the complex-valued coefficients a_ℓ^m are given by

$$a_\ell^m = \int_{\mathbb{S}_2} f(\mathbf{x}) Y_\ell^{m*}(\mathbf{x}) \Omega(d\mathbf{x}), \tag{4}$$

and the series (3) converges uniformly to f . Here and elsewhere we use $*$ to denote the complex conjugate.

Notice that the spherical harmonic $Y_0^0 = 1/\sqrt{4\pi}$, and thus $a_0^0 = 1/\sqrt{4\pi}$ is the normalizing constant for f . The series expansion (3) for a spherical density is analogous to the Fourier series expansion of a circular density; see, e.g., Eq. (2.1.5) in [30].

To replace the complex-valued Y_ℓ^m in the series expansion (3) by real spherical harmonics $Y_{\ell,m}$, the corresponding coefficients $a_{\ell,m}$ for the $Y_{\ell,m}$ are given in terms of a_ℓ^m by

$$a_{\ell,m} = \begin{cases} \{a_\ell^m + (-1)^m a_\ell^{-m}\} / \sqrt{2} & \text{if } m > 0, \\ a_\ell^0 & \text{if } m = 0, \\ \{a_\ell^{-m} - (-1)^m a_\ell^m\} / (i\sqrt{2}) & \text{if } m < 0, \end{cases}$$

and we have the alternate representation in terms of real harmonics:

$$f(\mathbf{x}) = \sum_{\ell=0}^{\infty} \sum_{m=-\ell}^{\ell} a_{\ell,m} Y_{\ell,m}(\mathbf{x}).$$

3. Some examples of spherical models and their series representation

We start by providing series representations in terms of spherical harmonics for a few commonly used spherical densities, namely the von Mises–Fisher, the Dimroth–Watson, a Brownian motion distribution, and the exponential family of spherical distributions. We also introduce in this section two new spherical models – see [Examples 5](#) and [6](#) – via their harmonics, and discuss their properties as we proceed.

Example 1. Consider the von Mises–Fisher (Fisher, Langevin) distribution [8,30]. The normalizing constant here involves the Modified Bessel function of the first kind I_ν , see (A.5), and the density is

$$f(\mathbf{x}; \boldsymbol{\mu}, \kappa) = \frac{\sqrt{\kappa}}{(2\pi)^{3/2} I_{1/2}(\kappa)} \exp(\kappa \boldsymbol{x}\boldsymbol{\mu}),$$

where $\kappa \geq 0$. The density function f on \mathbb{S}_2 depends on cosine of the angle say γ , between \mathbf{x} and $\boldsymbol{\mu}$, i.e., $\boldsymbol{x}\boldsymbol{\mu} = \cos(\gamma)$. The series expansion (3) can be seen to be

$$f(\mathbf{x}; \boldsymbol{\mu}, \kappa) = \sum_{\ell=0}^{\infty} \sqrt{\frac{2\ell + 1}{4\pi}} \frac{I_{\ell+1/2}(\kappa)}{I_{1/2}(\kappa)} Y_\ell^0(\boldsymbol{x}\boldsymbol{\mu}). \tag{5}$$

See [Appendix B.1](#) for a proof.

Example 2. The Dimroth–Watson distribution [36] has the density

$$f(\mathbf{x}; \boldsymbol{\mu}, \gamma) = \frac{1}{M(1/2, 3/2, \gamma)} \exp\{\gamma(\boldsymbol{x}\boldsymbol{\mu})^2\}, \tag{6}$$

where $M(1/2, 3/2, \gamma)$ is the Kummer function; see p. 181 in [23]. The series expansion (3) for this density can be shown to be

$$f(\mathbf{x}; \boldsymbol{\mu}, \gamma) = \sum_{\ell=0}^{\infty} c_{\ell} \sqrt{\frac{2\ell+1}{4\pi}} Y_{\ell}^0(\vartheta, \varphi) = \sum_{\ell=0}^{\infty} c_{\ell} \frac{2\ell+1}{4\pi} P_{\ell}(\cos \vartheta), \tag{7}$$

where $\vartheta = \arccos(\boldsymbol{\mu}\mathbf{x})$ with $c_{2\ell+1} = 0$ for the odd indices, and for the even indices

$$c_{2\ell} = \frac{2\pi}{M(1/2, 3/2, \gamma)} \int_{-1}^1 \exp(\gamma y^2) P_{2\ell}(y) dy. \tag{8}$$

See Appendix B.2 for a proof.

Example 3. Brownian Motion distribution, (see p. 174 in [23]) for which the series expansion (3) has the form

$$f(\mathbf{x}; \mathbf{x}_0, \zeta) = \sum_{\ell=0}^{\infty} e^{-\ell(\ell+1)/4\zeta} \frac{2\ell+1}{4\pi} P_{\ell}(\mathbf{x}_0\mathbf{x}), \tag{9}$$

where $\zeta > 0$; see Eq. (2).

Example 4. An exponential family of distributions for directional data was introduced in [4] and on p. 82 of [36]. Apart from the normalizing constant, the density has the form

$$f_{\ell}(\mathbf{x}) \propto \exp \sum_{\ell=0}^{\infty} \sum_{m=-\ell}^{\ell} c_{\ell}^m Y_{\ell}^m(\mathbf{x}),$$

where $c_{\ell}^{m*} = (-1)^m c_{\ell}^{-m}$. The normalizing constant corresponds to c_0^0 and depends on the rest of the parameters c_{ℓ}^m as well, since the integral of f_{ℓ} must be 1. Beran [4] uses the exponential of orthonormal spherical harmonics.

Apart from such familiar models, we note that for any given set (b_{ℓ}^m) of coefficients satisfying $\sum_{\ell=0}^{\infty} \sum_{m=-\ell}^{\ell} |b_{\ell}^m|^2 = 1$, one can indeed define a broad new class of densities by taking

$$f(\mathbf{x}) = \left| \sum_{\ell=0}^{\infty} \sum_{m=-\ell}^{\ell} b_{\ell}^m Y_{\ell}^m(\mathbf{x}) \right|^2.$$

Such a density can then be re-expressed in the general form (3), and the a_{ℓ}^n 's obtained explicitly from the Clebsch–Gordan series; see (A.3).

Two special cases of this are described in Examples 5 and 6, and are of particular interest. In quantum mechanics, the density represented by just the single term $Y_{\ell,m}(\mathbf{x})^2$ plays an important role in modeling the hydrogen atom.

Example 5. For $m > 0$, the density $Y_{\ell,m}^2$ has the representation of the form (3) as

$$Y_{\ell,m}^2 = \frac{2\ell+1}{2\sqrt{2\pi}} \sum_{h=m}^{\ell} \sqrt{\frac{1}{4h+1}} C_{\ell,0;\ell,0}^{2h,0} C_{\ell,m;\ell,m}^{2h,2m} Y_{2h,2m} + (-1)^m \frac{2\ell+1}{\sqrt{4\pi}} \sum_{h=0}^{\ell} \sqrt{\frac{1}{4h+1}} C_{\ell,0;\ell,0}^{2h,0} C_{\ell,m;\ell,-m}^{2h,0} Y_{2h,0}. \tag{10}$$

See Appendix B.3 for a proof.

The squared modulus $|Y_{\ell}^m(\mathbf{x})|^2$ provides yet another density function and serves as a model for rotationally symmetric densities on sphere, since the density function depends on the co-latitude via $\cos \vartheta$; compare Eqs. (1) and (21).

Example 6. The density $|Y_{\ell}^m|^2$ has a representation of the form (3), as

$$|Y_{\ell}^m|^2 = (-1)^m \frac{2\ell+1}{\sqrt{4\pi}} \sum_{h=0}^{\ell} \sqrt{\frac{1}{4h+1}} C_{\ell,0;\ell,0}^{2h,0} C_{\ell,m;\ell,-m}^{2h,0} Y_{2h}^0, \tag{11}$$

where $C_{\ell_1,m_1;\ell_2,m_2}^{k,m}$ are Clebsch–Gordan coefficients; see (A.3).

4. Mean direction and the moment of inertia

In this section, the mean direction and dispersion of any spherical model are expressed in terms of the harmonics.

4.1. Mean direction in terms of spherical harmonics

Representing a typical value of the random variable \mathbf{X} by $\mathbf{x} = (\sin \vartheta \cos \varphi, \sin \vartheta \sin \varphi, \cos \vartheta)^\top$, its mean is given by

$$\boldsymbol{\mu} = E(\mathbf{X}) = \int_{\mathbb{S}_2} \mathbf{x} f(\mathbf{x}) \Omega(d\mathbf{x}) = \int_{\mathbb{S}_2} \mathbf{x} \sum_{\ell=0}^{\infty} \sum_{m=-\ell}^{\ell} a_{\ell,m} Y_{\ell,m}(\mathbf{x}) \Omega(d\mathbf{x}). \tag{12}$$

We denote this mean vector by bold face $\boldsymbol{\mu}$ and note that $\boldsymbol{\mu} = E(\mathbf{X})$ is not necessarily a value on \mathbb{S}_2 . The entries of $\mathbf{x} = (\sin \vartheta \cos \varphi, \sin \vartheta \sin \varphi, \cos \vartheta)^\top$ can be expressed in terms of real spherical harmonics

$$x_1 = \sqrt{4\pi/3} Y_{1,1}, \quad x_2 = \sqrt{4\pi/3} Y_{1,-1}, \quad x_3 = \sqrt{4\pi/3} Y_{1,0}. \tag{13}$$

Using the orthogonality of spherical harmonics, we have the components of $\boldsymbol{\mu}$ as

$$\begin{aligned} \mu_1 &= \int_{\mathbb{S}_2} x_1 \sum_{m=-1}^1 a_{1,m} Y_{1,m}(\mathbf{x}) \Omega(d\mathbf{x}) = \sqrt{4\pi/3} a_{1,1}, \\ \mu_2 &= \sqrt{4\pi/3} a_{1,-1}, \quad \mu_3 = \sqrt{4\pi/3} a_1^0 = \sqrt{4\pi/3} a_{1,0}. \end{aligned}$$

Observe that although a_ℓ^m is complex-valued, μ_k is real and one can write

$$\boldsymbol{\mu} = R(\sin \vartheta_\mu \cos \varphi_\mu, \sin \vartheta_\mu \sin \varphi_\mu, \cos \vartheta_\mu)^\top = R\boldsymbol{\mu},$$

where the resultant length R is given by $R^2 = 4\pi(a_{1,1}^2 + a_{1,-1}^2 + a_{1,0}^2)/3$, and $\boldsymbol{\mu}$ is the mean direction. We remark that the mean direction depends on the first degree coefficients only and that $R \leq 1$.

Note that $R = 0$ for a uniform (isotropic) distribution, but it can also be zero for other non-uniform densities because of symmetries, as the following example illustrates.

Example 7 (Examples 5 and 6 Cont'd.). For both the densities $Y_{\ell,m}^2$ and $|Y_\ell^m(\mathbf{x})|^2$, we have $R = 0$ since there is no linear term in Clebsch–Gordan series; see (10) and (11), respectively.

4.2. Moment of inertia and the variance–covariance matrix in terms of spherical harmonics

We now discuss the second order moments and variance–covariance matrix which will be needed as we begin to consider the asymptotic distribution of the mean, and for estimating the rotational axes.

The product $\mathbf{x}\mathbf{x}^\top$ can be expressed in terms of real spherical harmonics, viz.

$$\mathbf{x}\mathbf{x}^\top = \sqrt{\frac{4\pi}{15}} \begin{bmatrix} Y_{2,2} & Y_{2,-2} & Y_{2,1} \\ Y_{2,-2} & -Y_{2,2} & Y_{2,-1} \\ Y_{2,1} & Y_{2,-1} & 0 \end{bmatrix} - \sqrt{4\pi/5} Y_{2,0} \text{diag}(1, 1, -2)/3 + \mathbf{I}/3,$$

where \mathbf{I} denotes the 3×3 identity matrix. Thus the moment of inertia depends only on the second degree coefficients and a constant. Notice that the trace of $\mathbf{x}\mathbf{x}^\top$ as well as of $E(\mathbf{X}\mathbf{X}^\top)$ is 1. The variance–covariance matrix is given by

$$\begin{aligned} \text{var}(\mathbf{X}) &= E(\mathbf{X}\mathbf{X}^\top) - E(\mathbf{X})E(\mathbf{X}^\top) \\ &= \sqrt{4\pi/15} \begin{bmatrix} a_{2,2} & a_{2,-2} & a_{2,1} \\ a_{2,-2} & -a_{2,2} & a_{2,-1} \\ a_{2,1} & a_{2,-1} & 0 \end{bmatrix} \\ &\quad - 4\pi \boldsymbol{\mu}_1/3 \boldsymbol{\mu}_1^\top - \sqrt{4\pi/45} a_{2,0} \text{diag}(1, 1, -2) + \mathbf{I}/3, \end{aligned} \tag{14}$$

where $\boldsymbol{\mu}_1^\top = (a_{1,1}, a_{1,-1}, a_{1,0})$.

Example 8 (Example 5 Cont'd.). For the density $Y_{\ell,m}^2$, $m > 0$, the series expansion (10) provides the following coefficients: $a_{0,0} = 1/\sqrt{4\pi}$, $a_{1,m} = 0$,

$$a_{2,0} = (-1)^m \frac{2\ell + 1}{\sqrt{20\pi}} C_{\ell,0;\ell,0}^{2,0} C_{\ell,m;\ell,-m}^{2,0}, \quad a_{2,2} = \delta_{m1} \frac{2\ell + 1}{\sqrt{40\pi}} C_{\ell,0;\ell,0}^{2,0} C_{\ell,1;\ell,1}^{2,2},$$

where δ_{mk} denotes the Kronecker delta, $a_{2,1} = a_{2,-1} = a_{2,-2} = 0$, (see p. 248 in [35]), hence $\text{var}(\mathbf{X})$ is diagonal. In particular, if \mathbf{X} has density $Y_{3,2}^2$, then $\text{var}(\mathbf{X}) = \mathbf{I}/3$, since $C_{3,2;3,-2}^{2,0} = 0$; see p. 252 in [35].

5. Estimation of the mean and covariances

For any inference and construction of tests based on a random a sample, one needs to consider estimating these harmonic coefficients and studying their properties, which is what we do next.

5.1. Estimation of a_ℓ^m

Consider now a random sample (iid observations) $\mathbf{x}_1(\vartheta_1, \varphi_1), \dots, \mathbf{x}_n(\vartheta_n, \varphi_n)$. Let the empirical density function $\bar{f}_n(\mathbf{x})$ be defined as usual by placing mass $1/n$ at each observation \mathbf{x}_k . The estimator $\widehat{a}_\ell^m, \ell \neq 0$, of a_ℓ^m given in (4) is

$$\widehat{a}_\ell^m = \int_{\mathbb{S}_2} \bar{f}_n(\mathbf{x}) Y_\ell^{m*}(\mathbf{x}) \Omega(d\mathbf{x}) = \frac{1}{n} \sum_{k=1}^n Y_\ell^{m*}(\mathbf{x}_k).$$

Clearly \widehat{a}_ℓ^m is unbiased since

$$E(\widehat{a}_\ell^m) = \frac{1}{n} \sum_{k=1}^n \int_{\mathbb{S}_2} f(\mathbf{x}) Y_\ell^{m*}(\mathbf{x}) \Omega(d\mathbf{x}) = a_\ell^m,$$

and has variance

$$\text{var } \widehat{a}_\ell^m = \frac{1}{n} (E|Y_\ell^m(\mathbf{X})|^2 - |a_\ell^m|^2),$$

where

$$E|Y_\ell^m(\mathbf{X})|^2 = (-1)^m \frac{2\ell + 1}{\sqrt{4\pi}} \sum_{h=0}^{\ell} \sqrt{\frac{1}{4h + 1}} C_{\ell,0;\ell,0}^{2h,0} C_{\ell,m;\ell,-m}^{2h,0} a_{2h}^0.$$

It also follows that \widehat{a}_ℓ^m is consistent. Using the convenient notation

$$P_{\ell_1,m_1}^{\ell_2,m_2} = E\{Y_{\ell_1}^{m_1}(\mathbf{X}) Y_{\ell_2}^{m_2}(\mathbf{X})^*\},$$

we may write

$$\text{cov}\{Y_{\ell_1}^{m_1}(\mathbf{X}), Y_{\ell_2}^{m_2}(\mathbf{X})\} = P_{\ell_1,m_1}^{\ell_2,m_2} - a_{\ell_1}^{m_1} a_{\ell_2}^{m_2*}. \tag{15}$$

This covariance can then be expressed in terms of the Clebsch–Gordan coefficients (see (A.3)),

$$P_{\ell_1,m_1}^{\ell_2,m_2} = (-1)^{m_2} \sum_{h=|\ell_1-\ell_2|}^{\ell_1+\ell_2} \sqrt{\frac{(2\ell_1 + 1)(2\ell_2 + 1)}{4\pi(2h + 1)}} C_{\ell_1,0;\ell_2,0}^{h,0} C_{\ell_1,m_1;\ell_2,-m_2}^{h,m_1-m_2} E\{Y_h^{m_1-m_2}(\mathbf{X})\},$$

resulting in the following

Lemma 1.

$$P_{\ell_1,m_1}^{\ell_2,m_2} = (-1)^{m_2} \sum_{h=|\ell_1-\ell_2|}^{\ell_1+\ell_2} \sqrt{\frac{(2\ell_1 + 1)(2\ell_2 + 1)}{4\pi(2h + 1)}} C_{\ell_1,0;\ell_2,0}^{h,0} C_{\ell_1,m_1;\ell_2,-m_2}^{h,m_1-m_2} a_h^{m_1-m_2}. \tag{16}$$

In the special case when the degrees match, i.e., $\ell_1 = \ell_2 = \ell$ and $2\ell + h$ is odd, then $C_{\ell,0;\ell,0}^{h,0} = 0$, and we obtain (see p. 250 in [35])

$$\begin{aligned} P_{\ell,m_1}^{\ell,m_2} &= (-1)^{m_2} \frac{2\ell + 1}{\sqrt{4\pi}} \sum_{h=0}^{2\ell} \sqrt{\frac{1}{2h + 1}} C_{\ell,0;\ell,0}^{h,0} C_{\ell,m_1;\ell,-m_2}^{h,m_1-m_2} a_h^{m_1-m_2} \\ &= (-1)^{m_2} \frac{2\ell + 1}{\sqrt{4\pi}} \sum_{h=0}^{\ell} \sqrt{\frac{1}{4h + 1}} C_{\ell,0;\ell,0}^{2h,0} C_{\ell,m_1;\ell,-m_2}^{2h,m_1-m_2} a_{2h}^{m_1-m_2}. \end{aligned}$$

Then

$$\text{cov}\{Y_\ell^{m_1}(\mathbf{X}), Y_\ell^{m_2}(\mathbf{X})\} = P_{\ell,m_1}^{\ell,m_2} - a_\ell^{m_1} a_\ell^{m_2*}$$

depends on the coefficients $a_{2h}^{m_1-m_2}$ with even degrees $2h \leq 2\ell$ and $a_\ell^{m_1} a_\ell^{m_2*}$.

5.2. A central limit theorem

For any given L , let \mathbf{A}_L denote the theoretical coefficients $\{a_\ell^m : \ell = 1, \dots, L, m = -\ell, \dots, \ell\}$ and $\widehat{\mathbf{A}}_L(n)$ be the corresponding vector of estimated coefficients obtained from the estimated $\{\widehat{a}_\ell^m : \ell = 1, \dots, L, m = -\ell, \dots, \ell\}$. Note that this $\widehat{\mathbf{A}}_L(n)$ is of dimension $L(L + 2)$, and is in general complex-valued except for the entries \widehat{a}_ℓ^0 with $\ell \in \{1, \dots, L\}$. From the Central Limit Theorem for empirical distributions (see, e.g., [11]), we note that $\widehat{\mathbf{A}}_L(n)$ is asymptotically complex Gaussian (CN), i.e.,

$$\sqrt{n} \{\widehat{\mathbf{A}}_L(n) - \mathbf{A}_L\} \rightsquigarrow \mathcal{CN}(0, \mathbf{C}), \tag{17}$$

where the elements of the covariance matrix \mathbf{C} are as defined in (15). An appropriate data-driven choice of L may be obtainable much as in Jupp [16], in any given context.

5.3. Estimation of the mean vector

A natural estimate of the mean direction $\boldsymbol{\mu}$, based on the sample $\mathbf{x}_1(\vartheta_1, \varphi_1), \dots, \mathbf{x}_n(\vartheta_n, \varphi_n)$ is the sample mean

$$\widehat{\boldsymbol{\mu}} = \bar{\mathbf{x}} = \frac{1}{n} \sum_{k=1}^n \mathbf{x}_k(\vartheta_k, \varphi_k).$$

It is easy to see that this estimator is equivalent to the one based on estimating a_1^m by \widehat{a}_1^m first, and then using formula (12) for getting $\widehat{\boldsymbol{\mu}}$. The variance of this estimator is given in terms of the variance–covariance matrix (14) and the asymptotic normality also follows from the result in (17). Estimating the variance–covariance matrix is also very similar and straightforward; see (14).

6. Rotations and different forms of spherical symmetry

Certain symmetries of physical systems, and in particular the rules of atomic spectroscopy, conservation of angular momentum, motivate one to consider the group of rotations of \mathbb{S}_2 , which forms a non-commutative group called $SO(3)$; see [37]. We follow the usual notation for a rotation $g \in SO(3)$ acting on a function f as $\Lambda(g)f(\mathbf{x}) = f(g^{-1}\mathbf{x})$. In particular $\Lambda(g)Y_\ell^m(\mathbf{x}) = Y_\ell^m(g^{-1}\mathbf{x})$, which is a rotated spherical harmonic, and is expressed in terms of other spherical harmonics in a natural manner in terms of Wigner D-matrices $D_{k,m}^{(\ell)}(g)$, i.e.,

$$\Lambda(g)Y_\ell^m(\mathbf{x}) = \sum_{k=-\ell}^{\ell} D_{k,m}^{(\ell)}(g)Y_\ell^k(\mathbf{x});$$

see Appendix A. Applying such a rotation on a density function f , we get

$$\begin{aligned} \Lambda(g)f(\mathbf{x}) &= \sum_{\ell=0}^{\infty} \sum_{m=-\ell}^{\ell} a_\ell^m \Lambda(g)Y_\ell^m(\mathbf{x}) \\ &= \sum_{\ell=0}^{\infty} \sum_{m=-\ell}^{\ell} a_\ell^m \sum_{k=-\ell}^{\ell} D_{k,m}^{(\ell)}(g)Y_\ell^k(\mathbf{x}) = \sum_{\ell=0}^{\infty} \sum_{k=-\ell}^{\ell} b_\ell^k(g)Y_\ell^k(\mathbf{x}), \end{aligned}$$

where the new coefficients $b_\ell^k(g)$ are transforms of a_ℓ^m as follows:

$$b_\ell^k(g) = \sum_{m=-\ell}^{\ell} a_\ell^m D_{k,m}^{(\ell)}(g). \tag{18}$$

We use this relationship to characterize symmetry of densities in particular cases.

6.1. Isotropy or uniformity on the sphere

One of the central problems in dealing with directional data, prior to any further inference, is to verify/test if the data are isotropic or uniformly distributed over \mathbb{S}_2 , in which case estimation of the mean or dispersion does not make sense.

Definition 1. f is isotropic (globally symmetric), if for all $g \in SO(3)$, $\Lambda(g)f(\mathbf{x}) = f(\mathbf{x})$.

This definition leads to the following necessary and sufficient condition for uniformity, and will be useful for inference.

Lemma 2. f is globally symmetric if and only if f is a uniform distribution on the sphere, i.e., $f(\mathbf{x}) = 1/(4\pi)$.

6.1.1. Testing uniformity or global symmetry

Testing uniformity is one of the well studied problems in circular statistics, and there are a large number of tests; see, e.g., Chapter 6 in [30]. More recently Rao Jammalamadaka et al. [29] provide another large-sample test that uses the Fourier coefficients for testing isotropy of circular data. A recent review of uniformity tests on the hypersphere can be found in [26]. In the case of the sphere, as noted before, the density f is globally symmetric or isotropic if and only if it has the form $f(\mathbf{x}) = 1/4\pi$ – in other words all coefficients a_ℓ^m are zero in the series expansion (3) except $a_0^0 = 1/\sqrt{4\pi}$. Thus we may re-state the null hypothesis of uniformity as

$$\mathcal{H}_0: a_\ell^m = 0, \text{ if } \ell \neq 0, \text{ for all } m.$$

Under this hypothesis, for any $\ell \neq 0$, $E(\widehat{a}_\ell^m) = 0$ with variance

$$\text{var}(\widehat{a}_\ell^m) = E|\widehat{a}_\ell^m|^2 - |E(\widehat{a}_\ell^m)|^2 = 1/(4\pi n).$$

This follows from

$$E|Y_\ell^m(\mathbf{x}_j)|^2 = P_{\ell,m}^{\ell,m} = Y_0^0/\sqrt{4\pi} = 1/(4\pi);$$

see (16). Using (A.4), we have

$$E\{Y_\ell^{m*}(\mathbf{x}_k)Y_\ell^m(\mathbf{x}_j)\} = \delta_{jk}1/(4\pi) + (1 - \delta_{jk})|a_\ell^m|^2 = \delta_{jk}1/(4\pi),$$

so that

$$E|\widehat{a}_\ell^m|^2 = \frac{1}{n^2} \sum_{k,j=1}^n E\{Y_\ell^{m*}(\mathbf{x}_k)Y_\ell^m(\mathbf{x}_j)\} = 1/(4\pi n).$$

Also, under \mathcal{H}_0 , if $\ell_1\ell_2 \neq 0$,

$$\text{cov}\{Y_{\ell_1}^{m_1}(\mathbf{x}_k), Y_{\ell_2}^{m_2}(\mathbf{x}_k)\} = \delta_{\ell_1\ell_2}\delta_{m_1m_2}/(4\pi),$$

while

$$n \text{cov}(\widehat{a}_{\ell_1}^{m_1}, \widehat{a}_{\ell_2}^{m_2}) = \delta_{\ell_1\ell_2}\delta_{m_1m_2}/(4\pi).$$

Thus $\widehat{a}_{\ell_1}^{m_1}$ and $\widehat{a}_{\ell_2}^{m_2}$ are uncorrelated if either $\ell_1 \neq \ell_2$, or $m_1 \neq m_2$.

The real and imaginary parts of the complex Gaussian variate have the same variance, which in our case is $1/(8\pi n)$. We have the same value for $|\widehat{a}_\ell^m| = |\widehat{a}_\ell^{-m}|$ provided $m \neq 0$. Hence the asymptotic distribution of $4\pi n(|\widehat{a}_\ell^m|^2 + |\widehat{a}_\ell^{-m}|^2)$ is a chi-square with 2 degrees of freedom, while $4\pi n|\widehat{a}_\ell^0|^2$ is asymptotically chi-square with 1 degree of freedom. Thus we have the following result.

Theorem 2. Under the above null hypothesis \mathcal{H}_0 of uniformity, we have

$$4\pi n \|\widehat{\mathbf{A}}_L(n)\|^2 = 4\pi n \sum_{\ell=1}^L \sum_{m=-\ell}^{\ell} |\widehat{a}_\ell^m|^2,$$

is asymptotically chi-square with $L(L + 2)$ degrees of freedom.

This statistic provides a nonparametric framework for testing uniformity on the sphere, and for the special case of $L = 1$, this test reduces to the Rayleigh test based on the length of the resultant; see [11]. Rewriting

$$\sum_{m=-\ell}^{\ell} |\widehat{a}_\ell^m|^2 = \frac{1}{n^2} \sum_{k,j=1}^n \frac{2\ell + 1}{4\pi} P_\ell(\mathbf{x}_k\mathbf{x}_j),$$

we get

$$4\pi n \|\widehat{\mathbf{A}}_L(n)\|^2 = \frac{1}{n} \sum_{k,j=1}^n \sum_{\ell=1}^L (2\ell + 1) P_\ell(\mathbf{x}_k\mathbf{x}_j).$$

and see that our test statistic is of the Beran type; see [3,27]. This approach of using the harmonic coefficients for testing uniformity on a sphere parallels that used in [29] for testing uniformity on the circle using Fourier coefficients.

6.2. Rotational symmetry

We now consider the issue of rotational symmetry with respect to a given axis $\mathbf{x}_0 = \mathbf{x}_0(\vartheta_0, \varphi_0)$.

Definition 2. f is rotationally symmetric about a given axis \mathbf{x}_0 if for any rotation $g \in SO(3)$, around axis \mathbf{x}_0 , $\Lambda(g)f(\mathbf{x}) = f(\mathbf{x})$.

For any given point \mathbf{x} , let γ denote the angle between this point and the axis of rotation, i.e., $(\mathbf{x}_0\mathbf{x}) = \cos \gamma$. We now show that a necessary and sufficient condition for such rotational symmetry is that f is a function of $\cos \gamma$ and satisfies (19).

Lemma 3. f is rotationally symmetric about the axis \mathbf{x}_0 if and only if $f(\mathbf{x}) = f(\mathbf{x}_0\mathbf{x}) = f(\cos \gamma)$ and has the particular form

$$f(\cos \gamma) = \sum_{\ell=0}^{\infty} c_\ell \frac{2\ell + 1}{4\pi} P_\ell(\cos \gamma). \tag{19}$$

Proof. Consider the tangent–normal decomposition of $\mathbf{x} \in \mathbb{S}_2$ given by

$$\mathbf{x} = \cos \gamma \mathbf{x}_0 + \sin \gamma \mathbf{y},$$

where \mathbf{y} is orthogonal to \mathbf{x}_0 , so that $\cos \gamma = \mathbf{x}_0 \mathbf{x}$. Now, f is rotationally symmetric about the axis \mathbf{x}_0 if and only if $f(\mathbf{x})$ does not depend on \mathbf{y} , i.e., $f(\mathbf{x}) = f(\cos \gamma) = f(\mathbf{x}_0 \mathbf{x})$. Recall the series expansion of $f(\cos \gamma)$ in terms of Legendre polynomials, viz.

$$f(\cos \gamma) = \sum_{\ell=0}^{\infty} b_{\ell} P_{\ell}(\cos \gamma).$$

If \mathbf{x}_0 is the North pole \mathbf{N} , then $\mathbf{N} \mathbf{x} = \cos \vartheta$ and using the fact $Y_{\ell}^0(\mathbf{x}) = \sqrt{(2\ell + 1)/4\pi} P_{\ell}(\cos \vartheta)$, we have

$$f(\mathbf{x}) = \sum_{\ell=0}^{\infty} b_{\ell} \sqrt{4\pi/(2\ell + 1)} Y_{\ell}^0(\mathbf{x}).$$

We compare this expansion to the one given in (3), obtaining $a_{\ell}^m = \delta_{m0} b_{\ell} \sqrt{4\pi/(2\ell + 1)}$. For later convenience, we will write

$$c_{\ell} = \sqrt{4\pi/(2\ell + 1)} a_{\ell}^0, \tag{20}$$

getting the expression (19).

6.2.1. Mean direction for a rotationally symmetric distribution

Let the rotation matrix M_{μ} be such that $M_{\mu} \boldsymbol{\mu} = \mathbf{N}$. Putting $\mathbf{x} = M_{\mu}^{-1} \mathbf{y}$, we find

$$E(\mathbf{X}) = \int_{\mathbb{S}_2} \mathbf{x} f(\mathbf{x} \boldsymbol{\mu}) \Omega(d\mathbf{x}) = M_{\mu}^{-1} \int_{\mathbb{S}_2} \mathbf{y} f(\mathbf{N} \mathbf{y}) \Omega(d\mathbf{y}) = c_1 M_{\mu}^{-1} \mathbf{N} = c_1 \boldsymbol{\mu},$$

since rotational axis of $f(\mathbf{N} \mathbf{y})$ is \mathbf{N} , $Y_{\ell}^0 \propto P_{\ell}$, and the result follows from (13). We see that the mean direction is $c_1 \boldsymbol{\mu}$, and since the rotational axis $\boldsymbol{\mu}$ is a unit vector, the resultant length $R = |c_1|$.

Example 9 (Example 6 Cont'd.). $|Y_{\ell}^m(\mathbf{x})|^2$ is written in Clebsch–Gordan series, in terms of spherical harmonics according to (3), (see (11))

$$|Y_{\ell}^m(\mathbf{x})|^2 = (-1)^m \frac{2\ell + 1}{4\pi} \sum_{h=0}^{\ell} C_{\ell,0;\ell,0}^{2h,0} C_{\ell,m;\ell,-m}^{2h,0} P_{2h}(\cos \vartheta). \tag{21}$$

Therefore $|Y_{\ell}^m(\mathbf{x})|^2$ is rotationally symmetric with respect to the axis \mathbf{N} , and the resultant is 0.

6.2.2. Moment of inertia for a rotationally symmetric distribution

As in the previous case,

$$E(\mathbf{X} \mathbf{X}^{\top}) = \int_{\mathbb{S}_2} \mathbf{x} \mathbf{x}^{\top} f(\mathbf{x} \boldsymbol{\mu}) \Omega(d\mathbf{x}) = M_{\mu}^{-1} \int_{\mathbb{S}_2} \mathbf{y} \mathbf{y}^{\top} f(\mathbf{N} \mathbf{y}) \Omega(d\mathbf{y}) M_{\mu}.$$

Substituting c_{ℓ} as defined in (20) into (14), the inertia matrix becomes

$$E(\mathbf{X} \mathbf{X}^{\top}) = M_{\mu}^{-1} \text{diag}(-c_2/3 + 1/3, -c_2/3 + 1/3, 2c_2/3 + 1/3) M_{\mu}.$$

Example 10 (Example 2 Cont'd.). The Dimroth–Watson distribution, see (6) and (8), has a moment of inertia equal to c_2 ; see (8).

Example 11 (Example 3 Cont'd.). The Brownian Motion distribution (9) has a moment of inertia given by $c_2 = e^{-3/2\zeta}$.

6.2.3. Estimation for rotationally symmetric distributions

We now consider estimation of the coefficients c_{ℓ} for a rotationally symmetric density

$$f(\cos \vartheta) = \sum_{\ell=0}^{\infty} c_{\ell} \frac{2\ell + 1}{4\pi} P_{\ell}(\cos \vartheta).$$

From Section 5.1 on the estimation of a_{ℓ}^m , it follows

$$\widehat{c}_{\ell} = \frac{1}{n} \sum_{k=1}^n P_{\ell}(x_{3,k}),$$

Table 1
Clebsch–Gordan coefficients and their simulated values.

ℓ	1	2	3	4
c_ℓ	0.000	0.297	0.000	0.058
\widehat{c}_ℓ	0.005	0.298	0.004	0.060
$\text{std}\{P_\ell(X_3)\}$	0.737	0.478	0.466	0.402
$\text{std}\{P_\ell(x_3)\}$	0.730	0.476	0.466	0.403

where $x_{3,k} = \cos \vartheta_k$, is the third component of observation \mathbf{x}_k . Thus $E(\widehat{c}_\ell) = c_\ell$, and for deriving the variance of \widehat{c}_ℓ we need an expression for $P_\ell(x_3)^2$ which is given by

$$P_\ell(x_3)^2 = \frac{4\pi}{2\ell + 1} Y_\ell^0(x_3)^2 = \sum_{0 \leq h \leq \ell} \sqrt{\frac{4\pi}{4h + 1}} (C_{\ell,0;\ell,0}^{2h,0})^2 Y_{2h}^0(x_3) = \sum_{0 \leq h \leq \ell} (C_{\ell,0;\ell,0}^{2h,0})^2 P_{2h}(x_3).$$

Now, one can write the variance of \widehat{c}_ℓ directly from the expectations of P_ℓ and P_ℓ^2 obtaining

$$n \text{ var } \widehat{c}_\ell = \text{var}\{P_\ell(X_3)\} = E\{P_\ell(X_3)^2\} - c_\ell^2 = \sum_{0 \leq h \leq \ell} (C_{\ell,0;\ell,0}^{2h,0})^2 c_{2h} - c_\ell^2. \tag{22}$$

Example 12. In this example, we illustrate how one might use a MATLAB function both for calculating the Clebsch–Gordan coefficients, as well as for simulating these values. For illustrative purposes, we consider the Dimroth–Watson distribution (7) with parameters $\gamma = 2$ and $\boldsymbol{\mu} = \mathbf{N}$. The coefficients c_ℓ and their standard deviations $\sqrt{\text{var } \widehat{c}_\ell}$ are calculated using formulas (8) and (22) respectively using MATLAB. A random sample $\mathbf{x}_1, \dots, \mathbf{x}_n$, with $n = 2^{12}$ is simulated using our MATLAB package “3D-Directional-SSV”; see [34] for details. Table 1 shows how close the calculated and simulated values are, for the first four coefficients.

6.2.4. Testing for rotational symmetry

We now consider testing the null hypothesis that the data come from a distribution which is rotationally symmetric around a given axis, which we can assume without loss of generality, is the North pole by rotating the specified axis to the North pole; see [9].

\mathcal{H}_0 : \mathbf{X} is rotationally symmetric around the North pole \mathbf{N} .

Under this hypothesis of rotational symmetry, f has the form (19), so that

$$E\{Y_\ell^{m*}(\mathbf{X})\} = c_\ell \delta_{m0} \sqrt{(2\ell + 1)/4\pi}.$$

Now, based on the observations $\mathbf{x}_1(\vartheta_1, \varphi_1), \dots, \mathbf{x}_n(\vartheta_n, \varphi_n)$, we know that \widehat{a}_ℓ^m is unbiased, viz. $E(\widehat{a}_\ell^m) = a_\ell^m$, and

$$E(\widehat{a}_\ell^m) = \delta_{m0} c_\ell \sqrt{(2\ell + 1)/4\pi}.$$

For the variance, appealing again to the Clebsch–Gordan series (16) with $m_1 m_2 \neq 0$, we recall $P_{\ell_1, m_1}^{\ell_2, m_2} = E\{Y_{\ell_1}^{m_1}(\mathbf{x}_j) Y_{\ell_2}^{m_2*}(\mathbf{x}_j)\}$, giving us

$$P_{\ell_1, m_1}^{\ell_2, m_2} = \frac{\delta_{m_1 m_2} (-1)^{m_1}}{4\pi} \sqrt{(2\ell_1 + 1)(2\ell_2 + 1)} \sum_{k=|m_1 - m_2|}^{\ell_1 + \ell_2} C_{\ell_1, 0; \ell_2, 0}^{k, 0} C_{\ell_1, m_1; \ell_2, -m_1}^{k, 0} C_k, \tag{23}$$

since $C_{\ell_1, m_1; \ell_2, -m_2}^{k, 0} = 0$, unless $m_1 - m_2 = 0$. Thus for $m_1 m_2 \neq 0$

$$\text{cov}\{Y_{\ell_1}^{m_1}(\mathbf{x}_j), Y_{\ell_2}^{m_2*}(\mathbf{x}_j)\} = \delta_{m_1 m_2} P_{\ell_1, m_1}^{\ell_2, m_1}.$$

Now we collect those \widehat{a}_ℓ^m which are uncorrelated and introduce the vector $\widehat{\mathbf{A}}_L(n)$ of estimated coefficients, viz.

$$\widehat{\mathbf{A}}_L(n) = (\widehat{a}_1^{-1}, \widehat{a}_1^1, \dots, \widehat{a}_L^{-L}, \widehat{a}_L^L)^\top.$$

This $\widehat{\mathbf{A}}_L(n)$ is complex-valued and is of dimension $2L$. We have $E\{\widehat{\mathbf{A}}_L(n)\} = \mathbf{0}$, and from (23) we have

$$nE|\widehat{a}_\ell^{\ell, \ell}|^2 = P_{\ell, \ell}^{\ell, \ell} = \frac{(-1)^\ell}{4\pi} (2\ell + 1) \sum_{k=0}^{\ell} C_{\ell, 0; \ell, 0}^{2k, 0} C_{\ell, \ell; \ell, -\ell}^{2k, 0} C_k.$$

Using (22), we get consistent estimates \widehat{c}_k of c_k for all $k \in \{0, \dots, \ell\}$, and plug them into $P_{\ell, \ell}^{\ell, \ell}$, leading to the following

Theorem 3. If \mathbf{X} is rotationally symmetric then $\widehat{\mathbf{A}}_\ell$ are uncorrelated and for large n ,

$$T_n = 2n \sum_{\ell=1}^L |\widehat{a}_\ell^\ell|^2 / P_{\ell,\ell}^{\ell,\ell} \sim \chi_{2L}^2.$$

We reject the null hypothesis if T_n is sufficiently large.

6.3. Other forms of symmetry

We now consider tests for various other types of symmetry that are not as well studied in the literature.

6.3.1. Axial or antipodal symmetry

Antipodal or axial symmetry refers to the density being the same at diametrically opposite ends, i.e., the densities at the points $\mathbf{x}(\vartheta, \varphi)$ and $\mathbf{x}(\pi - \vartheta, \varphi + \pi)$ are equal; see [5].

Definition 3. f is axially/antipodally symmetric, if $f(\mathbf{x}) = f(-\mathbf{x})$ for all $\mathbf{x} \in \mathbb{S}_2$.

For the “inversion” $\mathbf{x}(\vartheta, \varphi) \mapsto -\mathbf{x}(\pi - \vartheta, \pi + \varphi)$, we have

$$Y_\ell^m(-\mathbf{x}) = (-1)^\ell Y_\ell^m(\mathbf{x}). \tag{24}$$

If $f(\mathbf{x}) = f(-\mathbf{x})$, then

$$f(\mathbf{x}) = \sum_{\ell=0}^{\infty} \sum_{m=-\ell}^{\ell} a_\ell^m Y_\ell^m(\mathbf{x}) = f(-\mathbf{x}) = \sum_{\ell=0}^{\infty} \sum_{m=-\ell}^{\ell} (-1)^\ell a_\ell^m Y_\ell^m(\mathbf{x}),$$

from (24). Therefore $a_{2\ell+1}^m = -a_{2\ell+1}^m$, or $a_{2\ell+1}^m = 0$ for all m and ℓ . Thus we have the following characterization of such symmetry.

Lemma 4. f is axially symmetric if and only if for all ℓ and m , $a_{2\ell+1}^m = 0$, in which case the density has the form

$$f(\mathbf{x}) = \sum_{\ell=0}^{\infty} \sum_{m=-2\ell}^{2\ell} a_{2\ell}^m Y_{2\ell}^m(\mathbf{x}),$$

with mean direction $E(\mathbf{X}) = 0$.

Example 13 (Examples 5 and 6 Cont'd.). Both $Y_{\ell,m}^2$ (see (10)) and $|Y_\ell^m|^2$ (see (11)) are axially/antipodally symmetric.

6.3.2. Testing for axial symmetry

In this case as we noted before, the mean direction $E(\mathbf{X}) = 0$. For an observation vector $\mathbf{x}_1(\vartheta_1, \varphi_1), \dots, \mathbf{x}_n(\vartheta_n, \varphi_n)$, we have that \widehat{a}_ℓ^m is unbiased for a_ℓ^m . Therefore

$$E(\widehat{a}_{2\ell}^m) = a_{2\ell}^m, \quad E(\widehat{a}_{2\ell+1}^m) = 0.$$

We expect all $\widehat{a}_{2\ell+1}^m$ to be small. For calculating the covariance matrix of the estimators $\widehat{a}_{2\ell+1}^m$, consider first

$$P_{2\ell_1+1,m_1}^{2\ell_2+1,m_2} = (-1)^{m_2} \sum_{h=2|\ell_1-\ell_2|}^{2\ell_1+2\ell_2+2} \sqrt{\frac{(4\ell_1+3)(4\ell_2+3)}{4\pi(2h+1)}} C_{2\ell_1+1,0;2\ell_2+1,0}^{h,0} C_{2\ell_1+1,m_1;2\ell_2+1,-m_2}^{h,m_1-m_2} a_h^{m_1-m_2},$$

by (16). Since $2\ell_1 + 2\ell_2 + 2$ is even, so h must be even as well, giving us

$$P_{2\ell_1+1,m_1}^{2\ell_2+1,m_2} = (-1)^{m_2} \sum_{h=|\ell_1-\ell_2|}^{\ell_1+\ell_2+1} \sqrt{\frac{(4\ell_1+3)(4\ell_2+3)}{4\pi(4h+3)}} C_{2\ell_1+1,0;2\ell_2+1,0}^{2h,0} C_{2\ell_1+1,m_1;2\ell_2+1,-m_2}^{2h,m_1-m_2} a_{2h}^{m_1-m_2}.$$

Using the estimators $\widehat{a}_{2\ell+1}^m$ along with their covariance matrix in terms of $P_{2\ell_1+1,m_1}^{2\ell_2+1,m_2}$, one can construct a chi-square test statistic for checking the null hypothesis of axial symmetry.

6.3.3. Reflection with respect to the equatorial plane

Definition 4. f is symmetric with respect to equatorial plane ($\vartheta = \pi/2$), if for any $\mathbf{x}, \mathbf{x}' \in \mathbb{S}_2$, such that $\mathbf{x}(\vartheta, \varphi) \mapsto \mathbf{x}'(\pi - \vartheta, \varphi)$, then $f(\mathbf{x}) = f(\mathbf{x}')$.

This kind of symmetry is often observed, e.g., in crystallography and astrophysics, and is characterized as follows.

Lemma 5. f is symmetric with respect to the equatorial plane if and only if $a_{2\ell+1}^{2m} = 0$ and $a_{2\ell}^{2m+1} = 0$, for all ℓ and m , in which case the expansion has the form

$$f(\mathbf{x}) = \sum_{\ell=0}^{\infty} \left\{ \sum_{m=-\ell}^{\ell} a_{2\ell}^{2m} Y_{2\ell}^{2m}(\mathbf{x}) + \sum_{m=-\ell-1}^{\ell} a_{2\ell+1}^{2m+1} Y_{2\ell+1}^{2m+1}(\mathbf{x}) \right\}.$$

See Appendix B.4 for a proof.

Remark 1. The mean direction μ for a density which is symmetric with respect to the equatorial plane is $E(\mathbf{X}) = \sqrt{4\pi/3}(-a_{1,1}, a_{1,-1}, 0)^T$, and lies on the equatorial plane.

6.3.4. Testing for symmetry with respect to the equatorial plane

In this case, since the mean direction is given by $E(\mathbf{X}) = \sqrt{4\pi/3}(-a_{1,1}, a_{1,-1}, 0)^T$, we can test the hypotheses $a_{1,0} = 0$. As this is a necessary but not a sufficient condition for this type of symmetry, we need the following more elaborate procedure.

For an observation vector $\mathbf{x}_1(\vartheta_1, \varphi_1), \dots, \mathbf{x}_n(\vartheta_n, \varphi_n)$, we have that \hat{a}_ℓ^m is unbiased. Therefore,

$$E(\hat{a}_{2\ell+1}^{2m}) = 0, \quad E(\hat{a}_{2\ell}^{2m+1}) = 0, \tag{25}$$

so that we expect all $\hat{a}_{2\ell+1}^{2m}$ and $\hat{a}_{2\ell}^{2m+1}$ to be small. Again we can calculate the covariance matrix. By (16), we have

$$P_{\ell_1, m_1}^{\ell_2, m_2} = (-1)^{m_2} \sum_{h=|\ell_1-\ell_2|}^{\ell_1+\ell_2} \sqrt{\frac{(2\ell_1+1)(2\ell_2+1)}{4\pi(2h+1)}} C_{\ell_1,0;\ell_2,0}^{h,0} C_{\ell_1,m_1;\ell_2,-m_2}^{h,m_1-m_2} a_h^{m_1-m_2}.$$

Now if the parities of m_1 and m_2 are equal, then $m_2 - m_1$ is even, and if both ℓ_1 and ℓ_2 either odd or even then h should be even. If the parity of ℓ_1 and ℓ_2 is equal and at the same time the parity of m_1 and m_2 is also equal, then under (25) we have

$$\begin{aligned} P_{\ell_1, m_1}^{\ell_2, m_2} &= (-1)^{m_2} \sum_{h=|\ell_1-\ell_2|/2}^{(\ell_1+\ell_2)/2} \sqrt{\frac{(2\ell_1+1)(2\ell_2+1)}{4\pi(4h+1)}} C_{\ell_1,0;\ell_2,0}^{2h,0} C_{\ell_1,m_1;\ell_2,-m_2}^{2h,m_1-m_2} a_{2h}^{m_1-m_2} \\ &= \delta_{\ell_1\ell_2} \delta_{m_1m_2} / 4\pi. \end{aligned}$$

By contrast, if the parity of ℓ_1 and ℓ_2 are different, then h should be odd and $a_h^{m_1-m_2} \neq 0$; if $m_2 - m_1$ is odd, i.e., the parity of m_1 and m_2 are also different, then

$$P_{\ell_1, m_1}^{\ell_2, m_2} = (-1)^{m_2} \sum_{h=(|\ell_1-\ell_2|-1)/2}^{(\ell_1+\ell_2-1)/2} \sqrt{\frac{(2\ell_1+1)(2\ell_2+1)}{4\pi(4h+3)}} C_{\ell_1,0;\ell_2,0}^{2h+1,0} C_{\ell_1,m_1;\ell_2,-m_2}^{2h+1,m_1-m_2} a_{2h+1}^{m_1-m_2} = 0.$$

As before, based on the estimators $\hat{a}_{2\ell+1}^{2m}$ and $\hat{a}_{2\ell}^{2m+1}$, and the covariance terms, one can construct a chi-square test statistic for verifying the null hypothesis that \mathbf{X} is symmetric with respect to the equatorial plane.

7. Real data example: Sunspot activity

Solar photospheric activity is a long-standing subject of observation and research in astronomy. We consider data on Sunspots containing daily positions and areas of sunspots. These data are available at the Debrecen Photoheliographic Data (DPD) sunspot catalogue; see <http://fenyi.solarobs.csfk.mta.hu/DPD/> [2,12,13].

Locations of a spot refer to the position of the centroid of the whole spot or that of the umbra if an umbra is identified within a spot. Locations are defined by their Heliographic latitude and Heliographic longitude. We use daily data labeled “sDPD” and consider specifically four columns: Column No. 8 with NOAA sunspot group number, Column No. 9 with spot numbers within the group, Column No. 14 with Heliographic latitude which is positive: North, negative: South, and finally Column No. 15 with Heliographic longitude. The daily data contain the same spot as many times as its lifetime in days. We transformed the data so that each location is included only once. This way the data set between the years 1976–2014 included 187,223 positions, see Fig. 1.

The histogram of size 3072 shows two girdles equidistant from the equator; see Fig. 1. From this figure, we might surmise that a mixture of the Dimroth–Watson Distribution of the following form would provide a reasonable fit:

$$f(\mathbf{x}; \gamma, \alpha) \propto e^{\gamma \cos^2(\vartheta-\alpha)} / 2 + e^{\gamma \cos^2(\vartheta+\alpha)} / 2, \tag{26}$$

where $\alpha \in [0, \pi/2]$ and $\gamma < 0$. Here α moves the girdle up and down while $|\gamma|$ is the parameter of concentration. The model (26) can be considered as a particular case of a more general mixture of Dimroth–Watson Distributions, viz.

$$f_W(\mathbf{x}; \gamma, \alpha) \propto p e^{\gamma_1 \cos^2(\vartheta-\alpha_1)} + (1-p) e^{\gamma_2 \cos^2(\vartheta+\alpha_2)},$$

where $p \in [0, 1]$, $\alpha_1, \alpha_2 \in [0, \pi/2]$ and $\gamma_1, \gamma_2 < 0$. Simulating such a model is quite straightforward, starting with the simulation of two DW random variates with parameters γ_1, γ_2 , and then shift them by α_1, α_2 , respectively, and finally take a mixture with proportions p and $1 - p$.

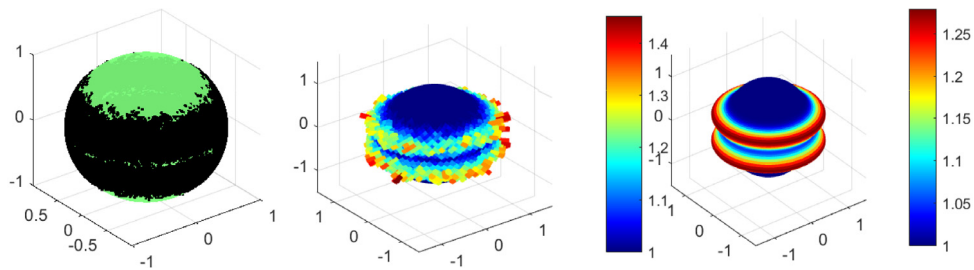


Fig. 1. From left to right: Sunspot data, the histogram and the fitted density.

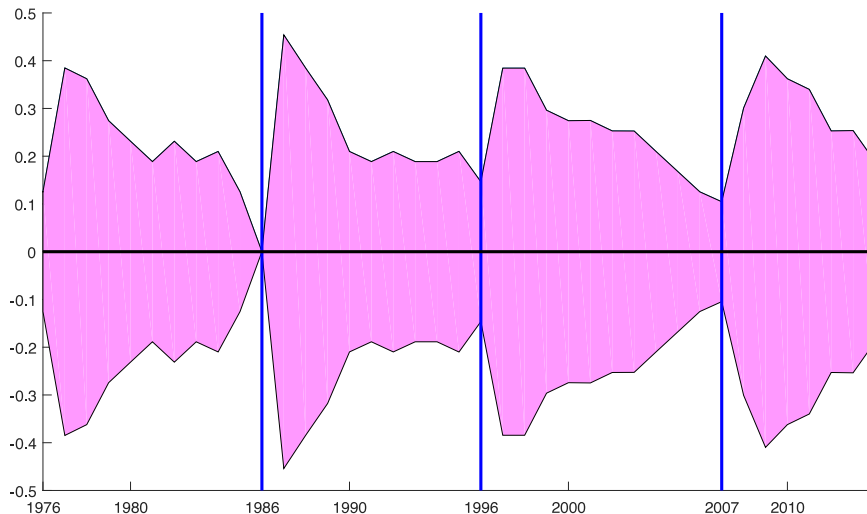


Fig. 2. The yearly estimated shift $\alpha, \hat{\alpha}(t)$ upper curve and $-\hat{\alpha}(t)$ lower curve, $t \in \{1976, \dots, 2014\}$.

We use the histogram $H(\mathbf{x})$ (see [34]), for estimating the parameter α in the model (26). First we take the average of $H(\mathbf{x})$ over the longitudes for each fixed co-latitude, maximum value over which gives an estimate $\hat{\alpha}$. For our data, this comes out to be $\hat{\alpha} = 0.2527$.

Now, for the given value of α , we estimate γ . Since the model (26) is rotationally symmetric with respect to the axis \mathbf{N} , the series expansion of the density has the form

$$f(\mathbf{x}; \gamma, \alpha) = \sum_{\ell=0}^{\infty} c_{2\ell}(\gamma, \alpha) \frac{2\ell + 1}{4\pi} P_{2\ell}\{\cos(\vartheta)\}.$$

We estimate the coefficients $c_{2\ell}(\gamma, \alpha)$ from the data for $\ell \in \{1, \dots, 10\}$, and apply the method of nonlinear least squares for fitting (26), obtaining $\hat{\gamma} = -39.0022$.

Remark 2. It is known that the Sunspot activity has a period of about 11 years, while a more precise period can be obtained using Carrington rotation numbers [12]. We estimated the shift α yearly between 1976 and 2014 and plotted both $\hat{\alpha}$ and $-\hat{\alpha}$. The period of roughly 11 years shows up in the “Butterfly” Fig. 2, which refers to the movement of girds (girds are the encircling bands of the distribution) by years.

Acknowledgments

We particularly thank the Chief Editor, Christian Genest, for the diligent reading and patient handling of this paper. We thank two anonymous referees for their valuable suggestions and detailed comments, that helped improve the paper significantly. This work was supported in part by the EFOP-3.6.2-16-2017-00015 project. The project has been supported by the European Union, cofinanced by the European Social Fund.

Appendix A. Legendre polynomials, spherical harmonics, the Funk–Hecke formula, and the Clebsch–Gordan series

Legendre polynomials. Legendre polynomials are the polynomial solutions to the so-called Legendre’s differential equation, and have several explicit representations, starting with $P_0(x) = 1, P_1(x) = x, P_2(x) = (3x^2 - 1)/2, \dots$. Standardized Legendre polynomials are orthogonal and satisfy

$$\int_{-1}^1 \{P_\ell(x)\}^2 dx = \frac{2}{2\ell + 1},$$

hence

$$\int_{\mathbb{S}_2} \{P_\ell(\cos \vartheta)\}^2 \Omega(d\mathbf{x}) = \frac{4\pi}{2\ell + 1}.$$

For more details, see, e.g., expression 2.17.5.1 in [28] and p. 180 in [7].

Spherical Harmonics. For any two points \mathbf{x}_1 and \mathbf{x}_2 on \mathbb{S}_2 , we have the addition formula

$$\sum_{m=-\ell}^{\ell} Y_\ell^{m*}(\mathbf{x}_1) Y_\ell^m(\mathbf{x}_2) = \frac{2\ell + 1}{4\pi} P_\ell(\cos \gamma), \tag{A.1}$$

where $\cos \gamma = \mathbf{x}_1 \mathbf{x}_2$; see p. 150 in [35].

Suppose G is continuous on $[-1, 1]$, then $G(\cos \gamma) = G(\mathbf{x}_1 \mathbf{x}_2)$ is defined on \mathbb{S}_2 , where \mathbf{x}_1 is fixed and $\mathbf{x}_1 \mathbf{x}_2 = \cos \gamma$. The series expansion in terms of Legendre polynomials, viz.

$$G(\cos \gamma) = \sum_{\ell=0}^{\infty} \frac{2\ell + 1}{2} \int_{-1}^1 G(x) P_\ell(x) dx P_\ell(\cos \gamma),$$

can be derived with the help of the Funk–Hecke formula which says (see p. 20 in [25])

$$\begin{aligned} \int_{\mathbb{S}_2} G(\mathbf{x}_1 \mathbf{x}_2) Y_\ell^m(\mathbf{x}_2) \Omega(d\mathbf{x}) &= G_\ell Y_\ell^m(\mathbf{x}_1), \\ G_\ell &= 2\pi \int_{-1}^1 G(x) P_\ell(x) dx. \end{aligned} \tag{A.2}$$

An important result that has been frequently used in this paper and which provides the coefficients for the product of two spherical harmonics $Y_{\ell_1}^{m_1}(\mathbf{x}) Y_{\ell_2}^{m_2}(\mathbf{x})^*$ in terms of linear combination of other spherical harmonics, is the so-called Clebsch–Gordan series (see p. 144 in [35]), and is given by

$$\begin{aligned} &Y_{\ell_1}^{m_1}(\mathbf{x}) Y_{\ell_2}^{m_2}(\mathbf{x})^* \\ &= (-1)^{m_2} \sum_{h=| \ell_1 - \ell_2 |}^{\ell_1 + \ell_2} \sqrt{\frac{(2\ell_1 + 1)(2\ell_2 + 1)}{4\pi(2k + 1)}} C_{\ell_1, 0; \ell_2, 0}^{k, 0} C_{\ell_1, m_1; \ell_2, -m_2}^{k, m_1 - m_2} Y_k^{m_1 - m_2}(\mathbf{x}). \end{aligned} \tag{A.3}$$

These quantities $C_{\ell_1, m_1; \ell_2, m_2}^{\ell, m}$ are called the Clebsch–Gordan coefficients and can be evaluated sometimes using available MATLAB codes. For some applications involving these for 3D spectra on sphere; see, e.g., [24,33].

Some basic properties that these coefficients satisfy are given by

$$\begin{aligned} \sum_{m_{1,2} = -\ell_{1,2}}^{\ell_{1,2}} C_{\ell_1, m_1; \ell_2, m_2}^{\ell, m} C_{\ell_1, m_1; \ell_2, m_2}^{\ell^*, m^*} &= \delta_{\ell \ell^*} \delta_{m m^*}, \\ C_{\ell_1, 0; \ell_2, 0}^{0, 0} &= \delta_{\ell_1 \ell_2} (-1)^{\ell_1} / \sqrt{2\ell_1 + 1}, \end{aligned}$$

and

$$C_{\ell_1, m_1; \ell_2, m_2}^{0, 0} = \delta_{m_1, -m_2} \delta_{\ell_1 \ell_2} (-1)^{\ell_1 - m_1} / \sqrt{2\ell_1 + 1} \tag{A.4}$$

and can be found on pages 250, 259 and 248, respectively, of [35].

Wigner D-matrices $D_{m,k}^{(\ell)}(g)$: (see p. 79 in [35] for more details). We introduce the notation $D^{(\ell)} = [D_{m,k}^{(\ell)}]$, for fixed rotation g . Thus $D^{(\ell)}$ denotes a unitary matrix of order $2\ell + 1$, and it follows $D^{(\ell)} [D^{(\ell)}]^{-1} = D^{(\ell)} D^{(\ell)*}$, $\det D^{(\ell)} = 1$ (unimodular). We shall use the integral

$$\int_{SO(3)} D_{m,k}^{(\ell)}(g) dg = \delta_{\ell 0} \delta_{m 0} \delta_{k 0},$$

where $dg = \sin \vartheta d\vartheta d\varphi d\gamma / 8\pi^2$ is the Haar measure; see I.4.14 in [31].

Modified Bessel function of the first kind I_ν (see 9.6.18 in [1]) is given by

$$I_\nu(z) = \frac{(z/2)^\nu}{\sqrt{\pi} \Gamma(\nu + 1/2)} \int_0^\pi e^{\pm z \cos \vartheta} \sin^{2\nu} \vartheta d\vartheta. \tag{A.5}$$

Appendix B. Some proofs

B.1. Harmonic series for Example 1

The Funk–Hecke formula, see (A.2), gives us

$$\int_{\mathbb{S}_2} f(\mathbf{x}\boldsymbol{\mu}; \kappa) Y_\ell^{m*}(\mathbf{x}) \Omega(d\mathbf{x}) = c_\ell Y_\ell^{m*}(\boldsymbol{\mu}),$$

where

$$c_\ell = 2\pi \int_{-1}^1 f(y; \kappa) P_\ell(y) dy.$$

Now

$$\int_{-1}^1 \exp(\kappa y) P_\ell(y) dy = \sqrt{2\pi/\kappa} I_{\ell+1/2}(\kappa),$$

hence $c_\ell = I_{\ell+1/2}(\kappa)/I_{1/2}(\kappa)$. Plugging in $c_\ell Y_\ell^{m*}$ into the series expansion (3) for f , we have

$$f(\mathbf{x}; \boldsymbol{\mu}, \kappa) = \sum_{\ell=0}^\infty \sum_{m=-\ell}^\ell c_\ell Y_\ell^{m*}(\boldsymbol{\mu}) Y_\ell^m(\mathbf{x}).$$

Finally applying the addition formula for the spherical harmonics, see (A.1), we obtain

$$f(\mathbf{x}; \boldsymbol{\mu}, \kappa) = \sum_{\ell=0}^\infty c_\ell \frac{2\ell + 1}{4\pi} P_\ell(\mathbf{x}\boldsymbol{\mu}) = \sum_{\ell=0}^\infty \frac{2\ell + 1}{4\pi} \frac{I_{\ell+1/2}(\kappa)}{I_{1/2}(\kappa)} P_\ell(\cos \gamma),$$

and using (2) gives us the desired result (5).

B.2. Harmonic series for Example 2

Again, using Funk–Hecke formula

$$\int_{\mathbb{S}_2} f(\boldsymbol{\mu}\mathbf{x}) Y_\ell^{m*}(\mathbf{x}) \Omega(d\mathbf{x}) = c_\ell Y_\ell^{m*}(\boldsymbol{\mu}),$$

where

$$c_\ell = \frac{2\pi}{M(1/2, 3/2, \gamma)} \int_{-1}^1 \exp(\gamma y^2) P_\ell(y) dy. \tag{B.1}$$

If ℓ is odd, then the integral vanishes since P_ℓ has the same parity as ℓ .

B.3. Harmonic series for Example 5

Note that for $m > 0$,

$$2Y_{\ell,m}^2 = \{Y_\ell^m + (-1)^m Y_\ell^{-m}\}^2 = (Y_\ell^m)^2 + (Y_\ell^{-m})^2 + 2|Y_\ell^m|^2,$$

and by Clebsch–Gordan series (A.3), we have

$$(Y_\ell^m)^2 = Y_\ell^m \{(-1)^m Y_\ell^{-m}\}^* = \frac{2\ell + 1}{\sqrt{4\pi}} \sum_{h=m}^\ell \sqrt{\frac{1}{4h + 1}} C_{\ell,0;\ell,0}^{2h,0} C_{\ell,m;\ell,m}^{2h,2m} Y_{2h}^{2m},$$

see [35], 8.5, (h), p. 250. Similarly $(Y_\ell^{-m})^2 = \{(Y_\ell^m)^2\}^*$ and

$$(Y_\ell^{-m})^2 = \frac{2\ell + 1}{\sqrt{4\pi}} \sum_{h=m}^\ell \sqrt{\frac{1}{4h + 1}} C_{\ell,0;\ell,0}^{2h,0} C_{\ell,m;\ell,m}^{2h,2m} Y_{2h}^{-2m},$$

which follows from $(Y_{\ell}^m)^2$. Therefore using (11) we have

$$Y_{\ell,m}^2 = \frac{2\ell + 1}{2\sqrt{4\pi}} \sum_{h=m}^{\ell} \sqrt{\frac{1}{4h+1}} C_{\ell,0;\ell,0}^{2h,0} C_{\ell,m;\ell,m}^{-2h,2m} (Y_{2h}^{2m} + Y_{2h}^{-2m}) \\ + (-1)^m \frac{2\ell + 1}{\sqrt{4\pi}} \sum_{h=0}^{\ell} \sqrt{\frac{1}{4h+1}} C_{\ell,0;\ell,0}^{2h,0} C_{\ell,m;\ell,-m}^{-2h,0} Y_{2h}^0,$$

and the required representation (10) follows.

B.4. Proof of Lemma 5

Consider the transformation $\mathbf{x}(\vartheta, \varphi) \mapsto \mathbf{x}'(\pi - \vartheta, \varphi)$, we have

$$Y_{\ell}^m(\pi - \vartheta, \varphi) = (-1)^{\ell+m} Y_{\ell}^m(\vartheta, \varphi).$$

Now using symmetry, we get

$$f(\mathbf{x}) = \sum_{\ell=0}^{\infty} \sum_{m=-\ell}^{\ell} a_{\ell}^m Y_{\ell}^m(\mathbf{x}) = f(\mathbf{x}') = \sum_{\ell=0}^{\infty} \sum_{m=-\ell}^{\ell} (-1)^{\ell+m} a_{\ell}^m Y_{\ell}^m(\mathbf{x}).$$

Using the fact that $a_{\ell}^m = (-1)^{\ell+m} a_{\ell}^m$, $a_{2\ell+1}^{2m} = 0$, and $a_{2\ell}^{2m+1} = 0$, we get

$$f(\mathbf{x}) = \sum_{\ell=0}^{\infty} \left\{ \sum_{m=-\ell}^{\ell} a_{2\ell}^{2m} Y_{2\ell}^{2m}(\mathbf{x}) + \sum_{m=-\ell-1}^{\ell} a_{2\ell+1}^{2m+1} Y_{2\ell+1}^{2m+1}(\mathbf{x}) \right\}.$$

References

- [1] M. Abramowitz, I.A. Stegun, Handbook of Mathematical Functions with Formulas, Graphs, and Mathematical Tables, Dover Publications Inc., New York, 1992, Reprint of the 1972 edition.
- [2] T. Baranyi, L. Györi, A. Ludmány, On-line tools for solar data compiled at the Debrecen observatory and their extensions with the Greenwich sunspot data, *Sol. Phys.* 291 (2016) 3081–3102.
- [3] R. Beran, Testing for uniformity on a compact homogeneous space, *J. Appl. Probab.* 5 (1968) 177–195.
- [4] R. Beran, Exponential models for directional data, *Ann. Statist.* (1979) 1162–1178.
- [5] C. Bingham, An antipodally symmetric distribution on the sphere, *Ann. Statist.* (1974) 1201–1225.
- [6] D.S. Chapman, H.N. Pollack, Global heat flow: A new look, *Earth Planet. Sci. Lett.* 28 (1975) 23–32.
- [7] A. Erdélyi, W. Magnus, F. Oberhettinger, F.G. Tricomi, Higher Transcendental Functions, Robert E. Krieger Publishing Co., Melbourne, FL, 1981.
- [8] R.A. Fisher, Dispersion on a sphere, *Proc. R. Soc. A* 217 (1953) 295–305.
- [9] E. García-Portugués, D. Paindaveine, T. Verdebout, On optimal tests for rotational symmetry against new classes of hyperspherical distributions, 2017, arXiv preprint arXiv:1706.05030.
- [10] M.G. Genton, S. Castruccio, P. Crippa, S. Dutta, R. Huser, Y. Sun, S. Vettori, Visuanimation in statistics, *Stat* 4 (2015) 81–96.
- [11] E. Giné, Invariant tests for uniformity on compact Riemannian manifolds based on Sobolev norms, *Ann. Statist.* 3 (1975) 1243–1266.
- [12] N. Gyenge, T. Baranyi, A. Ludmány, Variations of solar non-axisymmetric activity, *Central Eur. Astrophys. Bull.* 1 (2014) 1–16.
- [13] L. Györi, A. Ludmány, T. Baranyi, Comparative analysis of Debrecen sunspot catalogues, *Mon. Not. R. Astron. Soc.* 465 (2016) 1259–1273.
- [14] D.M. Healy, H. Hendriks, P.T. Kim, Spherical deconvolution, *J. Multivariate Anal.* 67 (1998) 1–22.
- [15] H. Hendriks, Nonparametric estimation of a probability density on a Riemannian manifold using Fourier expansions, *Ann. Statist.* 18 (1990) 832–849.
- [16] P.E. Jupp, Data-driven Sobolev tests of uniformity on compact Riemannian manifolds, *Ann. Statist.* 36 (2008) 1246–1260.
- [17] P.E. Jupp, B.D. Spurr, Sobolev tests for uniformity of directional data, *Ann. Statist.* 11 (1983) 1225–1231.
- [18] M. Kazhdan, B. Chazelle, D. Dobkin, T. Funkhouser, S. Rusinkiewicz, A reflective symmetry descriptor for 3D models, *Algorithmica* 38 (2004) 201–225.
- [19] P.T. Kim, J.-Y. Koo, H.J. Park, Sharp minimaxity and spherical deconvolution for super-smooth error distributions, *J. Multivariate Anal.* 90 (2004) 384–392.
- [20] S. Korman, R. Litman, S. Avidan, A. Bronstein, Probably approximately symmetric: Fast rigid symmetry detection with global guarantees, *Comput. Graph. Forum* 34 (2015) 2–13.
- [21] A.T.J. de Laat, R.J. van der A, M. van Weele, Tracing the second stage of ozone recovery in the Antarctic ozone-hole with a big data approach to multivariate regressions, *Atmos. Chem. Phys.* 15 (2015) 79–97.
- [22] C. Lacour, T.M.P. Ngoc, Goodness-of-fit test for noisy directional data, *Bernoulli* 20 (2014) 2131–2168.
- [23] K.V. Mardia, P.E. Jupp, Directional Statistics, Wiley, New York, 2009.
- [24] D. Marinucci, G. Peccati, Representations of SO(3) and angular polyspectra, *J. Multivariate Anal.* 101 (2010) 77–100.
- [25] C. Müller, Spherical Harmonics, Springer-Verlag, Berlin, 1966.
- [26] E.G. Portugués, T. Verdebout, An overview of uniformity tests on the hypersphere, 2018, arXiv preprint arXiv:1804.00286.
- [27] M.J. Prentice, On invariant tests of uniformity for directions and orientations, *Ann. Statist.* 6 (1978) 169–176.
- [28] A.P. Prudnikov, Y.A. Brychkov, O.I. Marichev, Integrals and series, in: Special Functions, Translated from the Russian by N.M. Queen, vol. 2, second ed., Gordon & Breach Science Publishers, New York, 1988.
- [29] S. Rao Jammalamadaka, S.G. Meintanis, T. Verdebout, Omnibus goodness of fit tests for uniformity of circular data, Technical Report, University of California, Santa Barbara, CA, 2017.
- [30] S. Rao Jammalamadaka, A. SenGupta, Topics in Circular Statistics, World Scientific, 2001.
- [31] E.M. Stein, G. Weiss, Introduction to Fourier Analysis on Euclidean Spaces, Princeton University Press, Princeton, NJ, 1971.
- [32] C. Sun, J. Sherrah, 3D symmetry detection using the extended Gaussian image, *IEEE Trans. Pattern Anal. Mach. Intell.* 19 (1997) 164–168.
- [33] Gy.H. Terdik, Angular spectra for non-Gaussian isotropic fields, *Braz. J. Probab. Stat.* 29 (2015) 833–865.
- [34] Gy.H. Terdik, S. Rao Jammalamadaka, B. Wainwright, Simulation and visualization of 3D-spherical distributions, Technical Report, University of California, Santa Barbara, CA, 2017.
- [35] D.A. Varshalovich, A.N. Moskalev, V.K. Khersonskii, Quantum Theory of Angular Momentum, World Scientific Press, 1988.
- [36] G.S. Watson, Statistics on spheres, in: University of Arkansas Lecture Notes in the Mathematical Sciences, Wiley, New York, 1983.
- [37] E.P. Wigner, Group Theory, and Its Application To the Quantum Mechanics of Atomic Spectra, Elsevier, 2012.